Published in final edited form as:
Nat Chem Biol. 2018 August ; 14(8): 760–763. doi:10.1038/s41589-018-0078-4.

Sarpagan bridge enzyme has substrate-controlled cyclization and aromatization modes

Thu-Thuy T Dang[#1], **Jakob Franke**[#1], **Inês Soares Teto Carqueijeiro**[2], **Chloe Langley**[1], **Vincent Courdavault**[2], and **Sarah E. O'Connor**[1,*]

[1]John Innes Centre, Department of Biological Chemistry, Norwich Research Park, Norwich NR4 7UH, UK

[2]Université François-Rabelais de Tours, EA2106 Biomolécules et Biotechnologies Végétales, Parc de Grandmont 37200 Tours, France

[#] These authors contributed equally to this work.

Abstract

Cyclization reactions that create complex polycyclic scaffolds are hallmarks of alkaloid biosynthetic pathways. We present the discovery of three homologous cytochromes P450 from three monoterpene indole alkaloid-producing plants (*Rauwolfia serpentina*, *Gelsemium sempervirens* and *Catharanthus roseus*) that provide entry into two distinct alkaloid classes, the sarpagans and the β-carbolines. Our results highlight how a common enzymatic mechanism, guided by related but structurally distinct substrates, leads to either cyclization or aromatization.

Monoterpene indole alkaloids (MIAs) are not only known for their potent biological activities, such as anticancer, anti-malarial and anti-arrhythmic properties1,2, but also for their complex polycyclic structures. Understanding and manipulating the underlying biosynthetic pathways of MIAs provides an effective way to access this medicinal treasure trove. One key cyclization reaction in MIA biosynthesis is catalyzed by sarpagan bridge enzyme (SBE) (Supplementary Fig. 1), a reaction that marks the entry of the central MIA intermediate strictosidine into sarpagan, ajmalan and alstophyllan alkaloid classes3, including the class Ia anti-arrhythmic agent ajmaline4 (**1**) and anticancer compound koumine5. Additionally, SBE is likely the gateway to certain oxindole alkaloids (*Gelsemium* spp.)6. Although enzymatic activity for SBE was detected in plant extracts over 20 years ago7, the corresponding gene has not been discovered. Here, we describe the discovery of two cytochrome P450 genes from *R. serpentina* and *Gelsemium sempervirens* that encode SBE activity, namely the conversion of strictosidine-derived geissoschizine (**2**) to the

sarah.oconnor@jic.ac.uk.

Contributions

T.T.T.D., J.F. and S.E.O. designed the experiments and wrote the manuscript. T.T.T.D. characterized RsSBE, GsSBE and CrAS *in vitro* and *in vivo*, performed *in planta* combinatorial assay and analysis. J.F. performed all substrate purification, synthesis and product characterizations. C.L. contributed to *N. benthamiana* work. I.S.T.C. and V.C. performed VIGS and localization experiments.

Competing Interests

The authors declare no competing financial interests.

Europe PMC Funders Author Manuscripts

sarpagan alkaloid polyneuridine aldehyde (PNA; **3**). Intriguingly, we demonstrate that SBE also aromatizes the tetrahydro-β-carboline alkaloids tetrahydroalstonine (**4**) and ajmalicine (**5**) to the corresponding β-carboline alkaloids alstonine (**6**) and serpentine (**7**) (Supplementary Fig. 1). We hypothesize that a shared iminium intermediate is responsible for the unusual connection of cyclization and aromatization reaction modes. We also demonstrate how the discovery of SBE now enables heterologous production of an ajmalan alkaloid.

We hypothesized that SBE is a cytochrome P450 that acts on geissoschizine (**2**), the product of a soluble reductase and strictosidine aglycone (**8**), the central intermediate of all MIA pathways (Supplementary Fig. 1) based on previous work on *R. serpentina* cell suspension cultures7 and recent work on strychnos-type MIA8. We conducted a co-expression analysis of publicly available *R. serpentina* transcriptome data9 using a self-organizing map10 (Supplementary Fig. 2). Additionally, we hypothesized that *G. sempervirens* should contain a homologous enzyme since sarpagan alkaloids, such as the anticancer compound koumine, have been reported from this plant6. Sequence data from the recently published *G. sempervirens* transcriptomes and genome11 revealed that two of the *R. serpentina* candidates selected from the self-organizing map (Rs_CYP_12057 and Rs_CYP_3375) have homologues with high sequence similarity (61 and 51% amino acid sequence identity) to *G. sempervirens* genes.

We used *Agrobacterium*-mediated transient expression in *Nicotiana benthamiana* to express SBE candidates. Since the expected PNA product may not be stable *in planta*, SBE candidates were expressed along with previously discovered pathway enzymes responsible for production of vinorine (**9**), which is derived from PNA and is a chemically stable intermediate in ajmaline biosynthesis (Fig. 1a). Thus, *N. benthamiana* was infiltrated with strictosidine (**10**) and *A. tumefaciens* strains encoding strictosidine glucosidase (SGD), geissoschizine synthase (CrGS, identified from *Catharanthus roseus*), polyneuridine aldehyde esterase (PNAE), vinorine synthase (VS) and SBE candidates for transient expression. To accelerate the screening process, up to three SBE candidates from *R. serpentina* and *G. sempervirens* were infiltrated simultaneously into *N. benthamiana*, and resulting plant tissue extracts were analyzed for the formation of vinorine. Liquid chromatography-mass spectrometry (LC-MS) analysis revealed the formation of vinorine (*m/z* 335) in plants that expressed one particular combination of SBE candidates in addition to SGD, CrGS, PNAE and VS (Fig. 1b). Deconvolution of this combination showed that it was Rs_CYP_12057, in the presence of SGD, CrGS, PNAE and VS, that was responsible for vinorine production (Fig. 1b).

We turned our attention to characterizing this SBE candidate more rigorously *in vitro*. However, geissoschizine is not available commercially, and CrGS primarily generates isositsirikine isomers8. Therefore, the related alkaloid geissoschizine methyl ether (**12**), together with structurally similar methyl ethers, were isolated from *Uncaria rhynchophylla*, which can be obtained as the Chinese drug Gou Teng12,13. These methyl ethers were chemically demethylated14 to provide milligram quantities of geissoschizine (Supplementary Fig. 3) and related compounds.

Next, CYP candidates were cloned into a yeast dual-expression vector that contained a cytochrome P450 reductase (CPR) to validate the *in planta* results. Geissoschizine (10 μM) was incubated with the yeast cultures for 24 hours. Only yeast cultures harboring the construct that encoded candidate Rs_CYP_12057 showed consumption of geissoschizine (*m/z* 353) and formation of a new product with *m/z* of 351 that had the same retention time and MS^2 fragmentation pattern as the synthetic PNA standard15 (Fig. 2a). No other candidate gene from *R. serpentina* utilized geissoschizine as a substrate. Although *R. serpentina* is not amenable to gene silencing, a silencing protocol has been developed for the related species, *Rauwolfia tetraphylla*, where ajmaline is also found in aerial organs16. Silencing of the *R. tetraphylla* SBE homolog (93% identity) led to a statistically significant decrease in ajmaline production, substantiating the physiological role of this gene in alkaloid biosynthesis (Supplementary Fig. 4). The homologue of Rs_CYP_12057 from *G. sempervirens* (Gs_207-0.13; 62% amino acid sequence identity) also converted geissoschizine to PNA (Fig. 2a). The identification of SBE from *G. sempervirens* provides the first biochemical evidence that PNA is potentially involved in the biosynthesis of *Gelsemium* alkaloids.

Rs_CYP_12057 and Gs_207-0.13, which are homologues, phylogenetically belong to the same clade as CYP71AY1 from *C. roseus* (78% amino acid sequence identity). All three proteins are members of the CYP71AY family (Rs_CYP_12057, CYP71AY4 and Gs_207-0.13, CYP71AY5, respectively; Supplementary Fig. 5). Rs_CYP_12057 shows the expected localization to the endoplasmic reticulum (Supplementary Fig. 6). Although *C. roseus* does not produce sarpagan or ajmalan alkaloids, CrCYP71AY1 converted geissoschizine to PNA, albeit with much lower efficiency (Fig. 2a), as shown in previous work with cell-free extract7. An empty-vector control exhibited no detectable PNA formation under the same conditions (Fig. 2a). Microsomal fractions of yeast expressing these genes (Supplementary Fig. 7) were used to biochemically characterize these enzymes. Rs_12057 and Gs_207-0.13 exhibited Michaelis-Menten kinetics with an apparent K_M value of 22.5 μM and 35.3 μM, respectively, for geissoschizine (Supplementary Fig. 8), while the activity of CrCYP71AY1 was so low that it could not be quantified accurately by steady-state kinetic assays. Due to the observed activity of Rs_CYP_12057 and Gs_207-0.13, these enzymes were named sarpagan bridge enzyme (SBE). Both *RsSBE* and *GsSBE* are highly expressed in root tissues, where the corresponding alkaloids are found in abundance, whereas *CrCYP71AY1* is primarily expressed in stem tissue (Supplementary Fig. 9). The discovery of SBE now corroborates the previously proposed reaction sequence geissoschizine to PNA.

As the C5-C16 bond formation of SBE is a crucial entry point into several alkaloid classes (Supplementary Fig. 1) and could potentially be harnessed to generate molecular complexity for other scaffolds, we tested the substrate specificity of these enzymes using a range of MIAs (Supplementary Fig. 10). Surprisingly, desmethylhirsuteine and desmethylhirsutine, two alkaloids differing from geissoschizine only in the ethylidene side chain, were not turned over, suggesting a crucial role of the 19*E* ethylidene group in promoting a conducive conformation for downstream cyclizations17. Intriguingly, two heteroyohimbine alkaloids, tetrahydroalstonine and ajmalicine, were turned over, resulting in formation of new products with a mass suggesting a four electron oxidation (Fig. 2b,c). The reaction products of

tetrahydroalstonine and ajmalicine were confirmed to be the corresponding fully aromatic β-carbolines, the anhydronium bases alstonine and serpentine, based on co-elution and MS^2 MRM fragmentation pattern with reference compounds (Supplementary Fig. 11). The β-carbolines have a variety of biological activities; for example, alstonine is used as a remedy to treat psychosis and other nervous system disorders18. Geissoschizine methyl ether (*m/z* 367.2) was also oxidized to a product with a mass decreased by 4 atomic units (*m/z* 363.2), suggesting oxidation to the β-carboline, though limited substrate availability and low catalytic activity hindered rigorous characterization of this oxidized product (Supplementary Fig. 11). CrCYP71AY1 exhibited Michaelis-Menten enzyme kinetics with a K_M of 19.6 μM for tetrahydroalstonine (Supplementary Fig. 8), and we designated this enzyme as alstonine synthase (AS). Collectively, these results highlight that all three SBE homologues from *R. serpentina*, *G. sempervirens* and *C. roseus* are, to a greater or lesser extent, capable of cyclization as well as aromatization reactions, depending on the identity of the starting substrate.

Our findings suggest a unifying mechanism for the action of SBE and the *C. roseus* homologue AS (Fig. 2c). We propose that SBE forms an iminium intermediate, by direct hydride abstraction or by step-wise oxidation, which can then follow two distinct reaction modes, cyclization or further oxidation. Cyclization occurs if a suitable nucleophile is correctly oriented to attack the iminium moiety. The side chain of geissoschizine (Fig. 2c), which exists primarily as the enol tautomer14,17, is an excellent nucleophile, allowing cyclization by a Mannich reaction, though an alternative radical mechanism cannot be ruled out. Alternatively, if no nucleophile is available for intramolecular cyclization (as in geissoschizine methyl ether, tetrahydroalstonine, or ajmalicine), the dihydropyridinium moiety that is generated by SBE could autoxidize spontaneously to the fully aromatic β-carboline, as has been previously observed in similar chemical systems19 (Fig. 2c). Earlier studies suggested a vacuolar peroxidase is responsible for the oxidation of ajmalicine20, and while we cannot exclude this possibility *in planta*, the shift in the substrate specificity of CrAS from geissoschizine to tetrahydroalstonine compared with RsSBE and GsSBE (Fig. 2a,b) supports a different biological role for CrAS. Moreover, the expression profile of *CrAS* (high in stem and roots) is in agreement with previous reports of β-carboline accumulation in *C. roseus* stem (and root) tissue20,21 (Supplementary Fig. 9). Such proposed function also illustrated how MIA-producing plants recruited and evolved the ADH/CYP71 biosynthetic module to synthesize strychnos, sarpagan and heteroyohimbine alkaloids. To explore the basis of the substrate specificity of CrAS, we made six point mutations based on sequence differences between CrAs and RsSBE that were also mapped onto a CYP homology model (Supplementary Fig. 12). Notably, PNA was produced by three CrAS mutants (S219A, E310W and V452I), suggesting that these residues are involved in mediating substrate recognition. This change in product profile suggests that these CYP71 enzymes may be amenable to protein engineering.

The indole alkaloids of the sarpagan–ajmalan type are found in approximately 100 plant species3. However, the biosynthetic gene leading to the intermediate PNA, at the crossroads of this pathway, has not been elucidated. Here we have shown how we rapidly identified this sarpagan bridge enzyme by combinatorial expression of ten CYP candidates in *N. benthamiana*, together with previously discovered pathway enzymes to push the production

towards a stable product that could serve as a readout for enzymatic activity. This approach demonstrates that combinatorial expression is a productive strategy for gene discovery and pathway reconstitution of ajmaline and other strictosidine-derived alkaloids when unstable substrates or products are involved. These homologous cytochromes P450 from the three alkaloid producer plants *R. serpentina*, *G. sempervirens* and *C. roseus* cyclize geissoschizine and thereby provide the entry point to sarpagan, ajmalan, alstophyllan and *Gelsemium* oxindole alkaloids. Moreover, these enzymes are capable of aromatizing alternative substrates to form β-carboline alkaloids. This discovery highlights how enzymatic promiscuity in substrate specificity, along with the inherent reactivity of these alkaloid substrates, can create a suite of structurally diverse chemical products.

Methods

Plants and chemicals

R. serpentina seeds were a gift from Dr. Subhash Hiremath, Karnataka University, India. The seeds were germinated at 28/22°C light/dark in a growth chamber with a photoperiod of 16 h. The 4-6 weeks plantlets were transferred to individual pots and grown in the greenhouse at the same temperature and light conditions. *G. sempervirens* seeds were obtained from Plant World Seeds UK and plants were grown in a greenhouse. *C. roseus* Little Bright Eyes cultivar was grown as reported earlier22. Polyneuridine aldehyde was a kind gift from Drs. E. Poupon and L. Evanno (Univ. Paris-Sud, CNRS, Université Paris-Saclay, France). Vinorine (**9**) was purchased from Northernchem Inc. (Niagara Falls, Ontario, Canada). Tetrahydroalstonine (**4**) was purchased from Extrasynthese (Lyon, France). Serpentine (**7**) was obtained from ChemFaces Biochemical Co.,Ltd. Alstonine was produced by oxidation of tetrahydroalstonine (**4**) with Pd black following a procedure by Younai et al.23 (NMR spectrum see Supplementary Fig. 3). Geissoschizine methyl ether and the related methyl ether alkaloids hirsuteine, hirsutine and rhynchophylline were isolated from *Uncaria rhynchophylla* and demethylated as described below. These are known compounds and ^{1}HNMR spectral data are provided. All other chemicals were of analytical grade from Sigma Aldrich.

Identification of cytochrome P450 (P450) candidates

Publicly available transcriptomic data of six different organs of *Rauwolfia serpentina* was filtered for contigs with FPKM (fragments per kilobase of exon per million fragments mapped) expression values higher than zero for more than half of the organs (i.e. transcripts with FPKM expression values of zero for more than half of the treatments or with zero expression variance across the samples were removed). Self-organizing maps were applied and visualized in R (RStudio 1.0.136, RStudio, Inc) with the Kohonen package24 as reported before10,22. The map was assigned to give about 50 contigs per node. Neighbouring nodes are related to each other by the similarity of their expression profile. The average expression profile of genes in the node is plotted within each node. To assess how well the generated self-organizing map fitted the data, two quality metrics were analyzed. The first was the within-node distance, which is defined as the mean distance from the weight vector of a node to the samples mapped to it. Therefore, the smaller the within-node distance, the more accurately the node's weight vector represents the samples mapped

to the node. The other quality metric used was the internodal distance, defined as the sum of the distances from a node's weight vector to the weight vectors of its neighbouring nodes. The smaller the value, the more similar a node's weight vector is to the weight vectors of its surrounding nodes. In order for a node to be classed as high quality in this analysis, both of the described quality metrics for that node had to be in the lowest quartile compared with all nodes. Cytochrome P450 candidates that are in the same nodes or neighbouring nodes with similar expression patterns as previously reported genes were selected for cloning and testing for activity.

Phylogenetic analysis

Unrooted neighbour-joining phylogenetic tree for CYP candidates from this study and other reported CYPs from other organisms were performed using the Geneious Tree Builder program in the Geneious software package (Geneious 8.1.8, Biomatters). Abbreviations and accession numbers of amino acid sequences used to generate phylogenetic tree: *R. serpentina* CYP 12057 (RsSBE, CYP71AY4, MF537711), *G. sempervirens* Gs207 (GsSBE, CYP71AY5, MF537712); *R. serpentina* CYP5437 (KY926696), *C. roseus* cytochrome P450 (CYP71D1V1) CrCYP71D1V1, AEX07770.1; *C. roseus* CrCYP71BT1, AHK60840.1; *C. roseus* CYP71AY1, CrCYP71Y1, AHK60849.1; *Solanum pennellii* isoflavone 2'-hydroxylase-like, SpFH, XM_015218869.1; *Theobroma cacao* cytochrome CYP71D9, Tc71D9, XP_017975886; *C. roseus* geraniol 10-hydroxylase, CrG10H, Q8VWZ7.1; *Nicotiana tabacum* CYP82M1v4, ABC69375.1; *C. roseus* CYP72A224 7-deoxyloganic acid 7-hydroxylase, Cr7DLH, AGX93062.1; *Papaver somniferum* cytochrome P450 CYP82X1, PsCYP82X1; AFB74614.1; *P. somniferum* cytochrome P450 CYP82Y1, PsCYP82Y1, AFB74617.1; *P. somniferum* cytochrome P450 CYP82X2, PsCYP82X2, AFB74617.1, AFB74616.1; *C. roseus* tabersonine 16-hydroxylase, CrCYP71D12, FJ647194.1; *Salvia miltiorrhiza* cytochrome P450 CYP82V2, SmCYP82V2, AJD25203.1; *C. roseus* secologanin synthase, CrSLS, Q05047.

Candidate gene screening and reconstitution of ajmalan pathway in *N. benthamiana*

The full-length coding regions of ADH and CYP candidates were amplified using cDNA derived from total root RNA of *R. serpentina* using Takara Ex Taq DNA polymerase (Clontech), and primer sets listed in Supplementary Table 1. For transient expression and candidate gene screening in *N. benthamiana*, the full-length coding regions were cloned into *BamH*I and *Kpn*I restriction sites of pTRBO25 using the In-fusion cloning system (Takara Clontech). pTRBO constructs were transformed into *Agrobacterium tumefaciens* GV3101 by electroporation. Transformants were selected on LB plates containing kanamycin, gentamicin and rifampicin. Cells were grown for 48 hrs at 28°C before harvested by centrifugation. The pellet was resuspended in infiltration buffer (10 mM NaCl, 1.75 mM $CaCl_2$, 100 μM acetosyringone) and incubated at room temperature for 2 hrs. *Agrobacterium* suspensions (OD_{600} = 0.1 for each strain) were infiltrated into the abaxial side of 5 week old *N. benthamiana* leaves with a needleless 1 mL syringe. *A. tumefaciens* strains encoding strictosidine glucosidase (SGD), geissoschizine synthase (GS, identified from *C. roseus*), polyneuridine aldehyde esterase (PNAE), vinorine synthase (VS) and up to 3 SBE candidates were mixed and infiltrated into *N. benthamiana* for transient expression. Substrate (50 μM) and caffeine standard (100 μM) were infiltrated into the leaves 3 days

post bacteria infiltration. Leaves were flash frozen in liquid N_2 and stored at –70°C before processing.

N. benthamiana metabolite extraction and analysis

Frozen leaf tissues were ground into powder in liquid N_2. 1000 μL of MeOH was added to each gram of tissue. The mixture was sonicated for 15 min and filtered before liquid chromatography-mass spectrometry (LC-MS) analysis. Elution of vinorine from combinatorial expression in *N. benthamiana* was monitored (multiple reaction monitoring, MRM) using four transitions *m/z* 335.2 > 243.2 (cone 36, collision 24), *m/z* 335.2 > 258.2 (cone 26, collision 32), *m/z* 335.1 > 275.2 (cone 36, collision 34), *m/z* 351.2 > 323.0 (cone 26, collision 16) on a Waters Acquity UPLC system (Milford, MA) coupled to a Xevo TQ-S mass analyzer.

Yeast expression vector construction

The full-length coding regions of CYP candidates were amplified using cDNA derived from total root RNA of *R. serpentina* using Takara Ex Taq DNA polymerase (Clontech), and primer sets listed in Supplementary Table 1. *GsSBE* was amplified from *G. sempervirens* root cDNA using the primers pESC-Leu2d-Gs207 fw/rv (Supplementary Table 1). *CrAS* was amplified from *C. roseus* stem cDNA using the primers pESC-Cr71AY1 (Supplementary Table 1). For heterologous expression of FLAG-tagged CYPs in yeast (*Saccharomyces cerevisiae*), the full-length coding regions of CYPs were cloned into *Spe*I restriction sites of the dual plasmid pESC-Leu2d::CPR26 yielding pESC-Leu2d::CYP/CPR using the In-fusion cloning system (Takara Clontech). The protease-deficient yeast strain YPL 154C:Pep4 KO strain27 was transformed with pESC-Leu2d::CYP/CPR. Yeast harboring pESC-Leu2d::CPR was used as the negative control.

Yeast culture, preparation of microsomes and immunoblot analysis

For routine yeast culture, the transgenic yeast strain was inoculated in 2 mL of synthetic complete (SC) medium lacking leucine (SC-Leu) containing 2% (w/v) glucose. The inoculum was cultured overnight at 30°C and 250 rpm. The culture was subsequently diluted 100-fold to an OD of 0.05 in SC-Leu supplemented with 2% (w/v) glucose and cultured for 16 h. Yeast was then harvested and sub-cultured for 24 h in SC-Leu containing 2% (w/v) galactose to induce recombinant protein production. Yeast cells were harvested by centrifugation and lysed in TES-B (0.6 M sorbitol in TE) using a Constant Systems cell disruptor at 35 kpsi and subsequently centrifuged at 11,000 *g* for 10 min at 4°C. The supernatant was then transferred to a new tube and centrifuged at 125,000 *g* for 90 min at 4°C. Finally, the pellet containing microsomes was resuspended with TEG buffer (20% (v/v) glycerol in TE). Recombinant enzymes were detected by immunoblot analysis using α-FLAG M2 (Genscript) detected with SuperSignal West Pico Chemiluminescent Substrate (ThermoFisher Scientific) (Supplementary Fig. 9).

Enzyme assays

Standard enzyme assays were performed at 30°C for 30 min in 100 μL of 100 mM HEPES-NaOH, pH 7.5, containing 0.1 mg of total microsomal proteins, 10 μM substrate and 100 μM

Europe PMC Funders Author Manuscripts

NADPH on a gyratory shaker with agitation (1000 rpm). Reactions were stopped by adding 800 μL methanol. A variety of alkaloids was used to test substrate specificity (see Supplementary Fig. 10, 11). The reaction mixture was extracted twice with methanol to precipitate and remove proteins. The supernatant was diluted with appropriate solvent for LC-MS/MS analysis. Steady-state enzyme kinetics was determined by varying the concentration of geissoschizine or tetrahydroalstonine between 0 and 300 μM at a fixed concentration of 200 μM NADPH (Supplementary Fig. 8). For quantification of alstonine and polyneuridine aldehyde, calibration curves were prepared and analyzed using eight calibration points in the range 0.006-0.08 ng/μL, in which the response was linear (R^2=0.98 for both compounds). Data processing was done using MassLynx 4.1 and TargetLynx software (Waters). Four transitions were used to monitor the elution of polyneuridine aldehyde: *m/z* 351.2 > 158.0 (cone 26, collision 21), *m/z* 351.2 > 166.0 (cone 26, collision 24), *m/z* 351.2 > 319.0 (cone 26, collision 19), *m/z* 351.2 > 323.0 (cone 26, collision 16). To monitor the elution of alstonine, four transitions were used: *m/z* 349.2 > 206 (cone 36, collision 50), *m/z* 349.2 > 234.9 (cone 36, collision 34), *m/z* 349.2 > 263.1 (cone 36, collision 30), *m/z* 349.2 > 317.1 (cone 36, collision 26). Kinetic constants were calculated by fitting initial velocity versus substrate concentration to the Michaelis-Menten equation using GraphPad Prism 5.0 (GraphPad Software). Data represent mean of three technical replicates.

LC-MS/MS analysis

Enzyme assays and alkaloid profiles of *N. benthamiana* plants were analysed by ultraperformance liquid chromatography (UPLC) on a Waters Acquity UPLC system (Milford, MA) coupled to a Xevo TQ-S mass analyzer. For kinetic studies, chromatography was performed on a BEH Shield RP_{18} (50 x 2.1 mm; 1.7 μm) column at a flow rate of 0.6 $mL.min^{-1}$. The column was equilibrated in solvent A (0.1% formic acid) and the following elution conditions were used: 0 min, 5% B (100% acetonitrile), from 0 to 3.5 min, 65% B; from 3.5 min to 3.75 min, 100% B; 3.75 min to 4.75, 100% B; 4.75 to 6 min, 5% B to re-equilibrate the column. Alternatively, the column was equilibrated in solvent A1 (0.1% NH_4OH) from 0 to 3.5 min, 65% B; from 3.5 min to 3.75 min, 100% B; 3.75 min to 4.75, 100% B; 4.75 to 6 min, 5% B to re-equilibrate the column. The basic mobile phase improves the peak shape of polyneuridine aldehyde.

Virus Induced Gene Silencing

Silencing of *RtSBE* in *R. tetraphylla* was achieved according to the procedure described in Corbin et al., (2017)16. The *RtSBE* silencing fragment was amplified with primers 5’-CTGAGAGGATCCTACTTGAAGCAGTTGCGCCAGATTTATGC-3’ and 5’-CTGAGAGGATCCAAGCACGGTGTCAAGTTGCTTCAAC-3’ and the resulting 362-bp gene fragment was cloned into pTRV2 to generate the pTRV2-viSBE silencing plasmid. Gene silencing was achieved by through the biolistic-mediated inoculation of viral vectors. Around four weeks post-transformation, leaves from four wild-type plants, three plants transformed with empty pTRV2 vector and five plants transformed with pTRV2-SBE were collected. Collected leaves were frozen in liquid nitrogen, powdered using a mixer mill (Retsch MM400) and subjected to LCMS according to Parage et al. (2016)28 (ajmaline m/z 327, RT=4.95 min; reserpilline *m/z* 413, RT=10.67 min) and qRT-PCR analysis using

primers 5'-CTCTATCATTTTGATTGGAAACTTCC-3' and 5'-TAGTTATCCTTATTCCACGACTCGA-3'. The sample size was 10 plants per condition (10 for SBE, 10 for empty vector and 10 for wild type; the transformation efficiency in *R. tetraphylla* is low16,29; the remaining plants were not effectively transformed). The experiment was repeated for a total of twice. Statistical analyses were performed with student T-Test (two-sided). Early biosynthesis steps in *Rauwolfia serpentina* occur in roots; even though we infected *R. tetraphylla* leaves, TRV-based vectors can spread systemically and are capable of silencing genes in roots, which might contribute to the strong reduction in ajmaline content.

Intracellular localization of SBE

Determination of the subcellular localization of Rs_SBE and Rt_SBE was performed by subcloning the full length coding sequences into the pSCA-cassette vector as YFP fusions. The nuclear (nucleus-CFP), nucleocytosolic (CFP) and endoplasmic reticulum (ER-CFP) markers were described previously30,31. Transient transformation of *C. roseus* cells by particle bombardment and fluorescence imaging were performed following the procedures previously described30,31. *C. roseus* cells were bombarded with DNA-coated gold particles (1 μm) and 1,100 psi rupture disc at a stopping-screen-to-target distance of 6 cm, using the Bio-Rad PDS1000/He system and 400 ng of each plasmid per transformation. Cells were cultivated for 16 h to 38 h before being harvested and observed. The subcellular localization was determined using an Olympus BX-51 epifluorescence microscope equipped with an Olympus DP-71 digital camera and a combination of YFP and CFP filters. Transformation was repeated three times and for each more than 100 transformed cells were observed. The CellD software (Olympus) was used to control the camera for photos and color attribution. Photos were cropped with Photo-Paint (Corel) to conserve only cells in the figure.

Isolation of geissoschizine methyl ether, hirsuteine, hirsutine and rhynchophylline

The methyl ether alkaloids geissoschizine methyl ether, hirsuteine, hirsutine and rhynchophylline were isolated from Gou Teng (Ramulus Uncariae cum Uncis), i.e. dried plant material of *Uncaria rhynchophylla* used in Traditional Chinese Medicine. Plant material was obtained from tcm4u.co.uk. 193 g of the dried woody plant material was ground in a blender to a fine powder and extracted 3x with 1 L ethanol, yielding 23.3 g of crude extract after concentrating *in vacuo*. The crude extract was dissolved in 250 mL 0.01 M HCl and washed with 300 mL EtOAc. The EtOAc layer was then re-extracted with 250 mL 0.01 M HCl. Both aqueous layers were combined, basified with 1 M NaOH to pH 8-9 and extracted 4x with 300-450 mL $CHCl_3$. The combined $CHCl_3$ layers were concentrated *in vacuo* to yield 0.47 g crude alkaloid extract. The crude alkaloid extract was separated on silica (50 g, 30-70 μm) using a step-wise gradient elution with $CHCl_3$/MeOH (95/5 (400 mL), 92/8, 90/10, 80/20, 70/30, 0/100; 200 mL each). Fractions containing the target compounds according to LCMS were separated by semipreparative HPLC on a Dionex Ultimate 3000 (Thermo Scientific) with UV detection at 254 nm using a BEH C_{18} OBD 130-5 column (250x10 mm, Waters XBridge) and a separation gradient (A: 0.1% NH_4OH in H_2O, B: acetonitrile, 40% to 70% B in 0 to 20 min) to give rhynchophylline (t_R = 11.7 min), hirsuteine (t_R = 12.6 min), hirsutine (t_R = 13.7 min) and geissoschizine methyl ether (t_R = 14.5 min). The identity of all compounds was confirmed by HRMS and NMR spectroscopy

in comparison with literature data. See Supplementary Fig. 3 for NMR spectra, references and Supplementary Table 2 and 3 for ^{1}H and ^{13}C data, respectively.

Demethylation of geissoschizine methyl ether, hirsuteine, hirsutine and rhynchophylline

Demethylation of methyl ether alkaloids was performed according to literature32. Typically, 0.1-3 mg substrate was dissolved in 80 μL AcOH and 20 μL conc. HCl was added. The mixture was incubated at RT for 2-3 days and monitored by MS for appearance of the demethylated product (– *m*/*z* 14). Afterwards, the reaction was quenched by slow addition of 400 μL 4 M K_2CO_3 and extracted 3x with 300 μL EtOAc. The combined organic layers were concentrated *in vacuo*, redissolved in methanol and purified by semipreparative HPLC on a Dionex Ultimate 3000 (Thermo Scientific) with UV detection at 254 nm using a BEH C_{18} OBD 130-5 column (250x10 mm, Waters XBridge) and a separation gradient (A: 0.1% NH_4OH in H_2O, B: acetonitrile, 25% to 55% B in 0 to 20 min) (geissoschizine: t_R = 7.5-8.6 min). The identity of geissoschizine was confirmed by HRMS and NMR spectroscopy in comparison with literature data14 (^{1}H NMR spectrum see Supplementary Fig. 3, ^{1}H NMR data see Supplementary Table 2, TopSpin (version 3.2) was used for analysis of NMR data).

RT-PCR of *GsSBE*

Expression of the *SBE* gene in *G. sempervirens* was tested by RT-PCR on cDNA obtained from RNA isolated from young leaves, old leaves, stem and roots. The aerial parts of 3-4 month old *G. sempervirens* plants were removed and separated into young leaves (bright green), old (mature) leaves (dark green), and stem. The remaining root ball was removed from soil, washed with tap water to remove soil particles and blotted dry. All tissues were flash frozen in liquid N_2 and ground in a mortar while frozen, until fine powders were obtained. Approximately 50 mg of each tissue was used for RNA extraction using the RNeasy Plant Mini kit (Qiagen) according to the manufacturer's instructions. RNA purity and quality was analyzed by spectrophotometry on a Nanodrop (Thermo Fisher) and agarose gel electrophoresis. cDNA synthesis was performed using the SuperScript III First-Strand Synthesis system (Thermo Fisher) with oligo$(dT)_{20}$ primers following the manufacturer's instructions. RT-PCR experiments were done using CloneAmp HiFi PCR premix (Clontech), 1 μL cDNA and 0.5 μL of each primer per 20 μL reaction. The primers GsSBE-RT fw/rv were used. As a positive control, primers designed for the homolog of the *7DLH* gene of *C. roseus*, 7DLH-RT fw/rv (Supplementary Table 1), were used.

Gene expression in different plant organs

Gene expression analysis was carried out using publicly available data for *C. roseus and R. serpentina*9.

Site-directed mutagenesis of CrAS

To probe which residues are responsible for the specificity of the reaction of CrAS and RsSBE, a homology model of CrAS and RsSBE was built based on allene oxide synthase33 (PDB ID: 3DAM, 13% amino acid identity with CrAS) using the Phyre2 web portal for protein modeling, prediction and analysis (Structural Bioinformatics Group, Imperial College, London). Sequence alignment of CrAS was then used to identify the regions where

sequence differences existed between the two proteins, and mapped them onto the homology model (Supplementary Figure 12). In most cases, the sequence changes were far from the putative heme and substrate binding sites. However, six mutations, including V125A, K211R, S219A, V308I, E310W, V452I, that are mostly on helices and loops that may be adjacent to the heme and substrate binding site of CrAS were created by overlap extension PCR as described before30. Mutant constructs were cloned into pESC-Leu2d and sequenced to verify the mutant gene sequence. Protein expression was confirmed by Western blot as described above. Enzyme assays were carried out with wildtype CrAS and other mutants as previously described.

Statistics and reproducibility

All information on statistical methods and reproducibility is shown in the corresponding figure legends.

Data Availability Statement

Gene sequences from this paper have been deposited to GenBank as: MF537711, *R. serpentina* CYP 12057 (RsSBE, CYP71AY4) and MF537712, *G. sempervirens* Gs_207-0.13 (GsSBE, CYP71AY5). *C. roseus* CYP71AY1 (CrAS, AHK60849.1) was deposited by ref. 34. All transcriptome data for *R. serpentina* and *C. roseus* are available at http://medicinalplantgenomics.msu.edu/.

Supplementary Material

Refer to Web version on PubMed Central for supplementary material.

Acknowledgements

T.T.T.D. is grateful to the EMBO Long Term Fellowship ALTF 739-2015. J.F. gratefully acknowledges DFG postdoctoral funding (FR 3720/1-1). This work was supported by grants from the European Research Council (311363), BBSRC (BB/J004561/1) (S.E.O.) and from the Région Centre, France (BioPROPHARM, CatharSIS grants) (V.C.). We thank Drs. Erwan Poupon and Laurent Evanno (Univ. Paris-Sud) for their generous gift of polyneuridine aldehyde standard. *Rauwolfia serpentina* seeds were a generous gift from Dr. Subhash Hiremath, Karnataka University, India. Dr. Dae-Kyun Ro generously provided pESC-Leu2d. Images of *R. serpentina* and *C. roseus* were provided by Dr. Tran Nguyen. We thank Dr. Lorenzo Caputi (John Innes Centre) for his assistance in building the homology model of CrAS and RsSBE and Drs. Lionel Hill and Gerhard Saalbach of the Molecular Analysis platform at John Innes Centre for their assistance in metabolic analysis.

References

1. O'Connor SE, Maresh JJ. Chemistry and biology of monoterpene indole alkaloid biosynthesis. Nat Prod Rep. 2006; 23:532–547. [PubMed: 16874388]
2. Cragg GM, Newman DJ. Natural products: A continuing source of novel drug leads. Biochim Biophys Acta - Gen Subj. 2013; 1830:3670–3695.
3. Namjoshi OA, Cook JM. Sarpagine and related alkaloids. Alkaloids Chem Biol. 2016; 76:63–169. [PubMed: 26827883]
4. Hashimoto Y, Hori R, Okumura K, Yasuhara M. Pharmacokinetics and antiarrhythmic activity of ajmaline in rats subjected to coronary artery occlusion. Br J Pharmacol. 1986; 88:71–77. [PubMed: 3708225]
5. Zhang X, et al. Apoptotic effect of koumine on human breast cancer cells and the mechanism involved. Cell Biochem Biophys. 2015; 72:411–6. [PubMed: 25561287]

6. Jin G-L, et al. Medicinal plants of the genus Gelsemium (Gelsemiaceae, Gentianales)--a review of their phytochemistry, pharmacology, toxicology and traditional use. J Ethnopharmacol. 2014; 152:33–52. [PubMed: 24434844]
7. Schmidt D, Stöckigt J. Enzymatic formation of the sarpagan-bridge: a key step in the biosynthesis of sarpagine- and ajmaline-type alkaloids. Planta Med. 1995; 61:254–258. [PubMed: 17238077]
8. Tatsis EC, et al. A three enzyme system to generate the Strychnos alkaloid scaffold from a central biosynthetic intermediate. Nat Commun. 2017; 8:316. [PubMed: 28827772]
9. Góngora-Castillo E, et al. Development of transcriptomic resources for interrogating the biosynthesis of monoterpene indole alkaloids in medicinal plant species. PLoS One. 2012; 7:e52506. [PubMed: 23300689]
10. Dang T-TT, Franke J, Tatsis E, O'Connor SE. Dual catalytic activity of a Cytochrome P450 controls bifurcation at a metabolic branch point of alkaloid biosynthesis in *Rauwolfia serpentina*. Angew Chem Int Ed Engl. 2017; 56:9440–9444. [PubMed: 28654178]
11. Stapleton JA, et al. Haplotype-Phased synthetic long reads from Short-Read Sequencing. PLoS One. 2016; 11:e0147229. [PubMed: 26789840]
12. Yuzurihara M, et al. Geissoschizine methyl ether, an indole alkaloid extracted from *Uncariae ramulus* et Uncus, is a potent vasorelaxant of isolated rat aorta. Eur J Pharmacol. 2002; 444:183–9. [PubMed: 12063078]
13. Yang Z, et al. Geissoschizine methyl ether, a corynanthean-type indole alkaloid from Uncaria rhynchophylla as potential acetylcholinesterase inhibitor. Nat Prod Res. 2011; 26:22–28. [PubMed: 21714741]
14. Takayama H, Watanabe T, Seki H, Aimi N, Sakai S. Geissoschizine revisited -definite proof of its stereostructure. Tetrahedron Lett. 1992; 33:6831–6834.
15. Ahamada K, Benayad S, Poupon E, Evanno L. Polyneuridine aldehyde: structure, stability overviews and a plausible origin of flavopereirine. Tetrahedron Lett. 2016; 57:1718–1720.
16. Corbin C, et al. Virus-induced gene silencing in Rauwolfia species. Protoplasma. 2017; 254:1813–1818. [PubMed: 28120101]
17. Eckermann R, Gaich T. The double-bond configuration of Corynanthean alkaloids and its impact on monoterpenoid indole alkaloid biosynthesis. Chemistry. 2016; 22:5749–55. [PubMed: 26933928]
18. Elisabetsky E, Costa-Campos L. The alkaloid alstonine: a review of its pharmacological properties. Evidence-Based Complement Altern Med. 2006; 3:39–48.
19. Korytowski W, Felix CC, Kalyanaraman B. Mechanism of oxidation of 1-methyl-4-phenyl-2,3-dihydropyridinium (MPDP+). Biochem Biophys Res Commun. 1987; 144:692–698. [PubMed: 3579936]
20. Blom TJ, et al. Uptake and accumulation of ajmalicine into isolated vacuoles of cultured cells of *Catharanthus roseus* (L.) G. Don. and its conversion into serpentine. Planta. 1991; 183:170–7. [PubMed: 24193617]
21. Singh D, et al. Predominance of the serpentine route in monoterpenoid indole alkaloid pathway of *Catharanthus roseus*. Proc Indian Natl Sci Acad. 2008; 74:97–109.
22. Payne RME, et al. An NPF transporter exports a central monoterpene indole alkaloid intermediate from the vacuole. Nat Plants. 2017; 16208:1–9.
23. Younai A, Zeng B, Meltzer HY, Scheidt KA. Enantioselective syntheses of heteroyohimbine natural products: a unified approach through cooperative catalysis. Angew Chem Int Ed Engl. 2015; 54:6900–4. [PubMed: 25914164]
24. Wehrens R, Buydens LMC. Self- and super-organizing maps in R: The kohonen package. J Stat Softw. 2007; 21:1–19.
25. Lindbo JA. TRBO: a high-efficiency tobacco mosaic virus RNA-based overexpression vector. Plant Physiol. 2007; 145:1232–40. [PubMed: 17720752]
26. Ro D, et al. Induction of multiple pleiotropic drug resistance genes in yeast engineered to produce an increased level of anti-malarial drug precursor, artemisinic acid. BMC Biotechnol. 2008; 8:83. [PubMed: 18983675]
27. Nguyen DT, et al. Biochemical Conservation and evolution of germacrene A oxidase in Asteraceae. J Biol Chem. 2010; 285:16588–16598. [PubMed: 20351109]

28. Parage C, et al. Class II Cytochrome P450 Reductase Governs the Biosynthesis of Alkaloids. Plant Physiol. 2016; 172:1563–1577. [PubMed: 27688619]
29. Valentine T, et al. Efficient virus-induced gene silencing in roots using a modified tobacco rattle virus vector. Plant Physiol. 2004; 136:3999–4009. [PubMed: 15591447]
30. Stavrinides A, et al. Structural investigation of heteroyohimbine alkaloid synthesis reveals active site elements that control stereoselectivity. Nat Commun. 2016; 7:1–14.
31. Guirimand G, et al. Optimization of the transient transformation of *Catharanthus roseus* cells by particle bombardment and its application to the subcellular localization of hydroxymethylbutenyl 4-diphosphate synthase and geraniol 10-hydroxylase. Plant Cell Rep. 2009; 28:1215–34. [PubMed: 19504099]
32. Koike T, Takayama H, Sakai S. Synthetic studies on the picraline-type indole alkaloids-I: improved synthesis of C-Mavacurine-type compounds and a new skeletal rearrangement in a corynanthe-type derivative. Chem Pharm Bull (Tokyo). 1991; 39:1677–1681.
33. Li L, Chang Z, Pan Z, Fu Z-Q, Wang X. Modes of heme binding and substrate access for cytochrome P450 CYP74A revealed by crystal structures of allene oxide synthase. Proc Natl Acad Sci. 2008; 105:13883–13888. [PubMed: 18787124]
34. Miettinen K, et al. The seco-iridoid pathway from *Catharanthus roseus*. Nat Commun. 2014; 5:3606. [PubMed: 24710322]

Europe PMC Funders Author Manuscripts

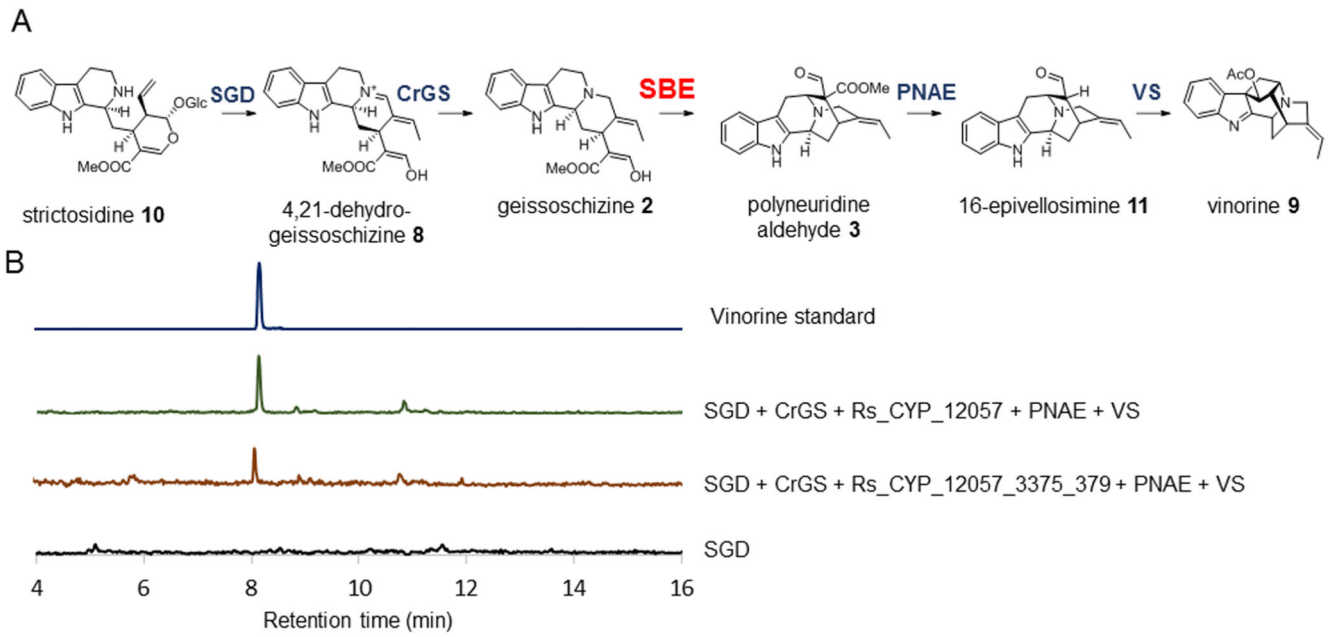

Figure 1. Sarpagan bridge enzyme candidate screening using combinatorial expression in *N. benthamiana*.

a, Biosynthetic pathway from strictosidine to the sarpagan alkaloid vinorine. 4,21-dehydrogeissoschizine is an isomer of strictosidine aglycone. **b**, Reconstitution of the biosynthetic pathway to vinorine from strictosidine in *N. benthamiana* to identify SBE. Multiple-reaction monitoring (MRM) chromatograms showing *in planta* catalytic activity of Rs_CYP_12057 in combination with strictosidine substrate and other known enzymes to produce vinorine (SGD + CrGS + Rs_CYP_12057 + Rs_CYP_3375 + Rs_CYP_379 + PNAE + VS and SGD + CrGS + Rs_CYP_12057 + PNAE + VS) compared with the negative control (SGD only). Experiments were repeated three times independently with similar results.

Europe PMC Funders Author Manuscripts

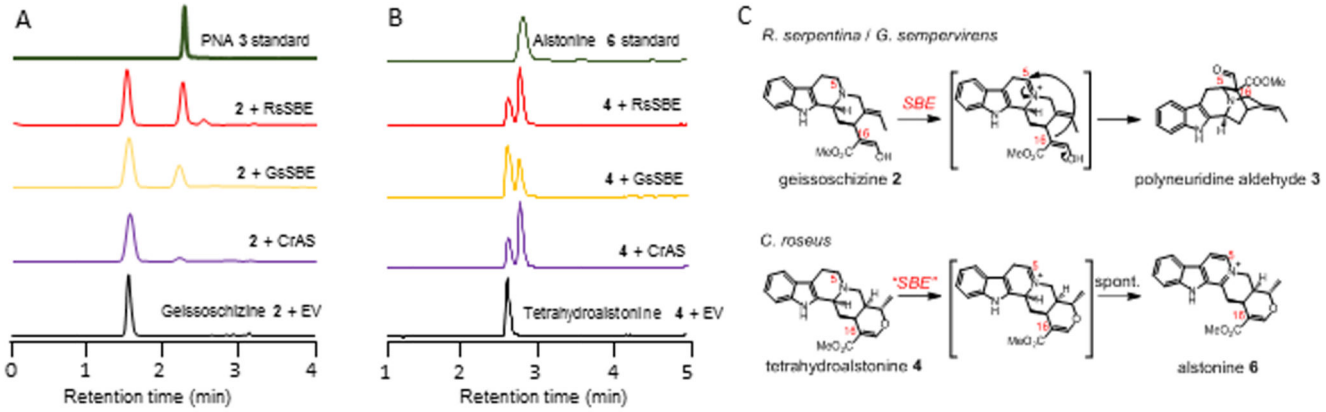

Figure 2. The cyclization and aromatization catalytic function of recombinant RsSBE, GsSBE and CrAS depend on the substrate.

a,**b**, MRM chromatograms showing the *in vivo* catalytic activity of RsSBE (Rs_CYP_12057), GsSBE (Gs_207-0.13) and CrAS (CrCYP71AY1) using geissoschizine (**2**; **a**) and tetrahydroalstonine (**4**; **b**) (*m/z* 353.2) as substrates compared with the empty vector negative control (EV). The identity of the trace side product in the geissoschizine + RsSBE reaction (red chromatogram) could not be determined. **c**, Proposed reaction mechanism for cyclization (upper panel) and aromatization (lower panel) with geissoschizine (**2**) and tetrahydroalstonine (**4**) via a common iminium intermediate. All experiments were repeated three times independently with similar results.

Europe PMC Funders Author Manuscripts